ELSEVIER

Ultrasound in Med. & Biol., Vol. 22, No. 9, pp. 1183–1190, 1996

0301-5629/96 $15.00 + .00

PII: S0301-5629(96)00167-6

●*Original Contribution*

A TWO-DIMENSIONAL EXTENSION OF MINIMUM CROSS ENTROPY THRESHOLDING FOR THE SEGMENTATION OF ULTRASOUND IMAGES

Y. ZIMMER,[†] R. TEPPER[‡] and S. AKSELROD[†]

[†]Medical Physics Department, Tel Aviv University, Tel Aviv, Israel;
and [‡]Department of Obstetrics and Gynecology, Sapir Medical Center, Kfar Saba, Israel

(*Received* 2 *February* 1996; *in final form* 5 *August* 1996)

Abstract—Segmentation is often an important step in medical image analysis. The local entropy is a possible variable for segmenting ultrasound images containing fluid surrounded by a soft tissue. A commonly used tool for image segmentation is thresholding. Recently, a new thresholding technique, known as "minimum cross entropy thresholding" (MCE), has been proposed. We present a multivariate extension of MCE in which the segmented variable (gray level) is replaced by a weighted combination of several image parameters. We propose to use a bivariate extension of MCE, which uses a linear combination of the gray level and the local entropy. The results obtained are demonstrated for ultrasound images of ovarian cysts.

Key Words: **Segmentation, Thresholding, Cross entropy, Image processing, Ultrasound.**

INTRODUCTION

Segmentation is often an important step in the analysis of medical images. The gray value of a pixel is the most widely used variable for region segmentation. Other features, such as the local texture, can also be utilized for that purpose. The local entropy, however, is considered more suitable for boundary extraction. Nevertheless, in ultrasound images containing transparent fluid encircled by soft tissue, it can be used for region segmentation.

Although much progress has been accomplished in automatic segmentation of medical ultrasound images, gynecological images have received relatively less attention. As an example, automatic segmentation applied on the ovaries can only rarely be found in the literature (Muzzolini et al. 1993; Muzzolini et al. 1994; Shinozuka et al. 1996).

From the early days of medical imaging, various thresholding approaches have been applied to segment medical images. Unlike in other imaging modalities, the gray levels in ultrasound images are not normally distributed. This fact makes the use of the well-known minimum error thresholding technique (Kittler and Illingworth 1986) inaccurate. Otsu's (1979) method, another widely used thresholding approach, is also inadequate in ultrasound since it provides a biased threshold when the gray level distribution functions have either unequal variances or populations.

Another important class of histogram-based thresholding algorithms are entropic methods. These techniques make use of the maximum entropy principle, originally discussed in information theory. The maximum entropy thresholding method proposed by Kapur et al. (1985) is considered superior to other algorithms. However, there are cases in which Kapur's method performs poorly. For example, a significantly overestimated threshold is obtained for ultrasound images containing a dark lumen (transparent fluid) encircled by a bright region (tissue). Recently, a new thresholding method, based on cross entropy, was suggested by Li and Lee (1993). This approach, known as "minimum cross entropy thresholding" (MCE), selects the threshold by minimizing the cross entropy between the original image and its segmented version. We have observed that usually MCE performs better than Kapur's algorithm in ultrasound images.

Brink and Pendock (1996) proposed a thresholding technique that is a variation of the method presented by Li and Lee (1993). They considered two alternative definitions of the cross entropy [the one

Address correspondence to: Solange Akselrod, Ph.D., Medical Physics Department, School of Physics and Astronomy, Tel Aviv University, Tel Aviv 69978, Israel. E-mail: Sol@novelty.tau.ac.il

used by Li and Lee (1993) and the one in which the roles of the original and the segmented images are reversed], and suggested to use either the latter one or their sum for thresholding. Using the sum introduces a symmetrical expression for the cross entropy. Since we found that Brink and Pendock's (1996) algorithm induced only slight changes in the obtained thresholds, we henceforth refer only to Li and Lee's (1993) method. Adapting our algorithm to the version proposed by Brink and Pendock (1996) is straightforward.

Although two-dimensional (2D) extensions of entropic methods have been suggested (Abutaleb 1989; Brink 1992), they were generally time consuming and suffered partly from the drawbacks of the one-dimensional (1D) algorithms from which they were derived.

We present a 2D extension of MCE, which uses a 1D summation. Hence, it is almost as fast as the original 1D MCE algorithm. Generalizations to a more sophisticated 2D extension and to a multivariate algorithm are also briefly discussed.

Combining the two components previously discussed—the local entropy and the 2D extension of MCE—we suggest a new scheme for segmentation of ultrasound images. In this approach, the gray levels of the pixels and their local entropies form a 2D histogram. This 2D parameter space is reduced to a 1D histogram, while assigning equal weights to both variables. Then, MCE is applied on the obtained histogram. The above 2D MCE algorithm is tested on several ultrasound images and the results are compared to those obtained using only the gray level (conventional MCE) or the local entropy. It is demonstrated that 2D MCE is usually a better way to separate transparent fluid from soft tissue in ultrasound images.

THE LOCAL ENTROPY

Definition

A medical ultrasonic image usually shows various tissues. Suppose we deal with a region-of-interest (ROI) representing a single tissue. Let us select from the image a small window containing N pixels located within the tissue. The probability of having a pixel with gray level g in the window is:

$$P_g = \frac{N_g}{N} \qquad (1)$$

where: N_g = the number of pixels with gray level g in the tissue and N = the total number of pixels in the window.

The local gray level entropy in the window can be defined as:

$$ENT = -\sum_{g=0}^{L} P_g \ln(p_g) \qquad (2)$$

where: L = the maximal possible gray level.

By definition, P_g describes the certainty that an arbitrary pixel has a gray level g. This certainty can be also measured by $ln(P_g)$. Ignoring the negative sign, eqn (2) provides in fact the average value of $ln(P_g)$ over all the possible values of g. Obviously, the average value of P_g (and hence, of $ln(P_g)$, too) is expected to be larger for a homogeneous local region than for a heterogeneous one, since the former contains less gray values. The local entropy is, therefore, smaller for a homogeneous region.

The above discussion indicates that the local entropy measures the homogeneity of the local region. Since the local entropy evaluates the gray level spreading in the histogram, it is related to the variance in the window and can be considered as a textural feature of the tissue.

Segmentation using the local entropy

In ultrasound images, the width of the local intensity histogram is correlated with its mean value. Such a correlation, which is related to the statistics of ultrasound speckle, has been previously demonstrated (Crawford et al. 1993; Karaman et al. 1995). As a consequence, a brighter region in the image exhibits a wider local gray level histogram and vice versa. The local entropy, which evaluates the width of the histogram, is therefore correlated with the local brightness.

It may seem odd to use the local entropy for region segmentation. This variable is considered much more suitable for boundary extraction, since near boundaries it usually occupies much higher values than inside regions; the large values of the local entropy near a boundary are caused by the variety of gray levels (related to both sides of the border) included in the window. In the context of medical imaging, this description fits computerized tomography and magnetic resonance images. In ultrasound images, unlike the former modalities, the local gray level histogram far from a boundary may spread over a range as wide as the histogram at the interface between two different tissues (each using the entire set of gray levels bounded by the histogram). Hence, the local entropies within and between tissues may be similar. This fact reduces the effectiveness and reliability of boundary extraction based on the entropy in ultrasound images.

Using the local entropy for region segmentation is possible because the local entropy is correlated with the local brightness. Generally, the quality of tissue discrimination is dependent on the contrast between the tissues. When an image contains regions representing water or another transparent fluid encircled by a soft

tissue, regions representing fluid appear dark and demonstrate a narrow gray level distribution while regions representing soft tissue appear bright and have a much wider intensity distribution. In such cases, the local entropy of "fluid" is significantly smaller than the one of "soft tissue." Therefore, the local entropy can be used to differentiate between these two kinds of tissues in ultrasound images.

MINIMUM CROSS ENTROPY THRESHOLDING

The notion of cross entropy was proposed by Kullback (1959). The cross entropy, which measures the information theoretic distance between two distributions $P = \{p_1, p_2, \ldots, p_N\}$ and $Q = \{q_1, q_2, \ldots, q_N\}$, is expressed by:

$$D(Q, P) = \sum_{k=1}^{N} q_k \log_2\left(\frac{q_k}{p_k}\right) \tag{3}$$

Recently, Li and Lee (1993) suggested a new thresholding method based on cross entropy, which is known as minimum cross entropy thresholding (MCE). In their method, the probability q_k is formed by dividing the gray level of the kth pixel in the original image (assuming the image contains N pixels) to the sum of the gray levels in all the image pixels. Similarly, the probability p_k is generated from the kth pixel in the segmented image (i.e., the binary image obtained after thresholding). These probability distributions are better understood if an image is viewed as an array of cells which is illuminated. The gray level at each cell then represents the number of photons reaching that cell. Hence, dividing each value by the total number of photons will provide the relative illumination at each cell. The above model, which provides an intuitive explanation for the choice of probability distributions, is discussed by Brink and Pendock (1996).

The two gray levels that are used in the segmented image (one value for all the pixels below the threshold and the other value for the rest) can generally depend on the threshold. Li and Lee (1993) used $\mu_1(t)$ and $\mu_2(t)$ [which are defined in eqn (4)], as the gray levels of the pixels below and above the threshold t, respectively. Under this assumption, it can be shown that the cross entropy is proportional to the following expression (Li and Lee 1993):

$$\eta(t) = \sum_{j=1}^{t-1} jh_j \ln\left(\frac{j}{\mu_1(t)}\right) + \sum_{j=t}^{L} jh_j \ln\left(\frac{j}{\mu_2(t)}\right) \tag{4}$$

where:

$$\mu_1(t) = \frac{\sum_{j=0}^{t-1} jh_j}{\sum_{j=0}^{t-1} h_j},$$

$$\mu_2(t) = \frac{\sum_{j=t}^{L} jh_j}{\sum_{j=t}^{L} h_j},$$

and

h_j = the no. of pixels having gray level j.

Obviously, minimizing $\eta(t)$ is equivalent to minimizing the cross entropy between the original image and its segmented version. Hence, the optimal threshold is the value of t that minimizes $\eta(t)$.

TWO-DIMENSIONAL MCE

We have previously seen that the thresholding criterion in MCE is given by:

$$\eta(t) = \sum_{j<t} jh_j \ln\left(\frac{j}{\mu_1(t)}\right) + \sum_{j\geq t} jh_j \ln\left(\frac{j}{\mu_2(t)}\right) \tag{5}$$

We would now like to generalize this expression to a 2D parameter space while maintaining the 1D summation. A possible form of such generalized equation may be:

$$\eta(t) = \sum_{K(i,j)<t} K(i,j) h_{K(i,j)} \ln\left(\frac{K(i,j)}{\mu_1(t)}\right) + \sum_{K(i,j)\geq t} K(i,j) h_{K(i,j)} \ln\left(\frac{K(i,j)}{\mu_2(t)}\right). \tag{6}$$

$K(i,j)$ is symmetric with respect to i,j and reduces to the 1D expression when only one variable is considered.

Since the formal values of i and j affect the value of K, we assume for simplicity that both variables occupy the same range of possible values.

In order to find good candidates for $K(i,j)$ we will analyze the problem from a geometrical point of view. We know that eqn (5) describes a sum over a 1D vector. In fact, each element in the sum is associated with a cell whose distance from the origin is j. The obvious generalization to 2D should involve an elementary "cell" in the 2D matrix whose distance from the origin (i.e., radius) is $K(i,j)$. Two candidates

for $K(i,j)$, which have simple geometrical meaning, can be suggested:

$$K_1(i,j) = i + j, \tag{7}$$

and

$$K_2(i,j) = \sqrt{i^2 + j^2}\,. \tag{8}$$

In the first case, the sum is computed on straight lines obeying i + j = C, while in the second case, the sum is computed on circular rings obeying $\sqrt{i^2 + j^2} = C$.

Figure 1 demonstrates how the computation is performed in both cases. In each part of the figure, the filled area represents the part of the parameter space in which $K(i,j) < C$ (for a specific value of C) while the empty area shows the rest of the matrix. The curve shows the matrix elements for which the distance from the origin is C.

Let us now consider the function $K(i,j)$ as a new variable k, and construct its histogram. Obviously, each cell in this histogram will contain a contribution only from a unique line or ring (depending on the case) in the 2D matrix. Hence, the 2D parameter space was reduced to a 1D histogram of the variable k. Using eqn (6), it is easy to see that the thresholding criterion for k is given by:

$$\eta(t) = \sum_{k<t} kh_k \ln\left(\frac{k}{\mu_1(t)}\right) + \sum_{k\geq t} kh_k \ln\left(\frac{k}{\mu_2(t)}\right) \tag{9}$$

where:

$$\mu_1(t) = \frac{\sum_{k<t} kh_k}{\sum_{k<t} h_k}, \quad \mu_2(t) = \frac{\sum_{k\geq t} kh_k}{\sum_{k\geq t} h_k}.$$

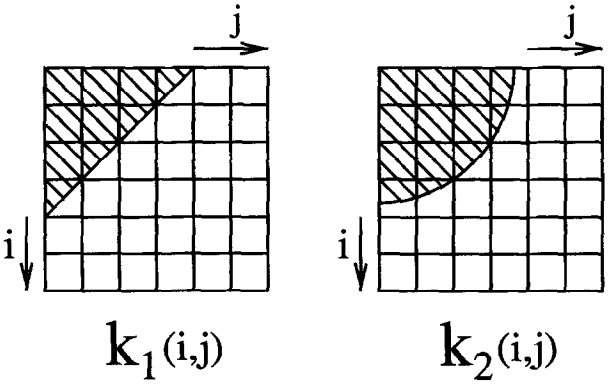

Fig. 1. Partition of the 2D parameter space by a specific value of $K(i,j)$.

We see that the regular 1D criterion for MCE is obtained. Hence, we can apply regular MCE on the histogram of k and find a threshold. If the curve in Fig. 1 signifies $K(i,j) = t$ (where t is the obtained threshold), the pixels in the filled region would be below the threshold while the rest would be above it.

The entire process can be viewed as clustering. Since the pixels from each tissue form a cluster in the parameter space, the curve $K(i,j) = t$ can be viewed as a decision curve separating the clusters. Clustering is performed using the cross entropy as a metric, and $\eta(t)$ as the expression to be minimized.

GENERALIZATIONS

Generalization to unequal weights

So far, $K(i,j)$ was limited to functions symmetric with respect to i and j. However, this special case can be generalized to functions of the form:

$$K_1(i,j) = a \cdot i + b \cdot j, \tag{10}$$

and

$$K_2(i,j) = \sqrt{a^2 i^2 + b^2 j^2}\,. \tag{11}$$

These equations, in which each variable is preceded by a coefficient, can be viewed as combinations of i and j with nonequal weights. Equations (7) and (8) represent the special case in which equal weights are used. By selecting the coefficients, the user can determine the relative importance of each variable in the thresholding process.

It is desired to keep the values of $K(i,j)$ in the range of i's and j's, so that t does not become multiplied by an arbitrary factor. Hence, the expression for $K(i,j)$ must be normalized. The new coefficients should be defined as true weights (i.e., their sum must be 1). Hence, the normalized version of eqns (10) and (11), respectively, will be:

$$K_1(i,j) = w_1 i + w_2 j \tag{12}$$

where

$$w_1 = \frac{a}{a+b}, \quad w_2 = 1 - w_1 = \frac{b}{a+b};$$

and

$$K_2(i,j) = \sqrt{w_1^2 i^2 + w_2^2 j^2}\,. \tag{13}$$

where:

$$w_1^2 = \frac{a^2}{a^2 + b^2}, \quad w_2^2 = 1 - w_1^2 = \frac{b^2}{a^2 + b^2}.$$

It should be noticed that in order for eqns (12) and (13) to be reduced to eqns (7) and (8), respectively, when equal weights are used, eqn (12) should be multiplied by 2, and eqn (13) should be multiplied by $\sqrt{2}$.

From a geometrical point of view, eqn (12) means summing on straight lines with a general slope (instead of lines with slope -1) and eqn (13) means summing on elliptical rings (instead of circular rings). It follows that the decision curve between the two clusters in the parameter space is either a line with a predetermined slope or an elliptical arc. Any knowledge about the shapes of the two clusters may be used to optimize the weights, in order to obtain a better decision curve.

Generalization to multivariate thresholding

Until now, the discussion was restricted to bivariate thresholding. However, it may be desired to consider several different variables for segmentation. The modification of eqns (12) and (13), respectively, for multivariate thresholding is:

$$K_1(x_1,x_2,\ldots,x_N) = \sum_{i=1}^{N} w_i x_i \qquad (14)$$

where:

$$\sum_{i=1}^{N} w_i = 1;$$

and

$$K_2(x_1,x_2,\ldots,x_N) = \sqrt{\sum_{i=1}^{N} w_i^2 x_i^2} \qquad (15)$$

where:

$$\sum_{i=1}^{N} w_i^2 = 1.$$

In this case the decision curve is replaced by a decision surface. This surface can be either a plane or an ellipsoid.

Generalization to other thresholding methods

This article discusses a 2D extension of MCE. In principle, the same idea can be applied to other thresholding techniques. A general scheme for thresholding would be:

1. Construct $K(x_1,x_2,\ldots,x_N)$ using the selected set of variables and coefficients.
2. Sort the pixels in the image according to their k value.
3. Find the threshold for k using the desired thresholding method.
4. Segment the image.

COMBINING THE LOCAL ENTROPY WITH 2D MCE

Multivariate MCE can be applied using any set of variables. We have chosen to focus on the 2D case, where the pair of variables are the gray level and the local entropy. The motivation for using the local entropy was its relative robustness to gray level variations. We have tested both straight and elliptic decision curves [eqns (12) and (13), respectively], but were soon convinced that the simpler selection (straight line) was sufficient. Thus, we concentrated on implementing 2D MCE where the variable $K(i,j)$ is determined by a linear combination of the gray level and the local entropy.

We have also tried other parameter sets, but neither using more than two variables simultaneously nor selecting another pair significantly improves the results. Nevertheless, specific conditions for which such improvement may occur, should be further investigated.

RESULTS AND DISCUSSION

We have applied 2D MCE using eqn (12) on several ultrasound images containing ovarian cysts (fluid) encircled by ovarian tissue (soft tissue). We have tried various weights for the intensity and local entropy, and discovered that, when the fluid does not contain significant noise, equal weights are sufficient. It was also evident that the original method proposed by Li and Lee (1993) frequently failed to segment these images satisfactorily. We have compared the results obtained for equal weights to those formed when zero weight was given either to the gray level or to the local entropy. The later case (zero weight to the local entropy) is easily identified as the conventional MCE technique.

The images presented in this article were obtained using the Aloka SSD-680 scanner (Aloka, Tokyo, Japan) with a 5-MHz transvaginal probe with 128 channels. The images were recorded on video cassettes, and later digitized into the computer.

For each image we selected a ROI, which contained only the two relevant tissues, and performed all computations on this ROI. We have tested various sizes of windows for computing the local entropy of each pixel, and discovered that good results are obtained in the range 7×7 to 15×15 pixels. Hence, in this study

Fig. 2. Segmentation results for an ovarian cyst with transparent fluid (example 1). Top left = original image; top right = segmentation using the local entropy; bottom left = segmentation using the gray level (conventional MCE); bottom right = segmentation using both variables (2D MCE).

a window size of 11 × 11 pixels was selected and such are the results hereby presented.

Figures 2–4 provide examples of the results obtained when the tested images are composed of transparent fluid (dark fluid without bright noise) and soft tissue. Each figure contains four images: top left, the original image; top right, the segmented image formed considering only the local entropy; bottom left, the segmented image generated considering only the gray level (conventional MCE); bottom right, the segmented image obtained using equal weights (2D MCE).

It can be concluded from these figures that conventional MCE sometimes yields reasonable results (e.g., Fig. 4), but in many occasions the threshold is significantly overestimated (e.g., Fig. 2–3). Hence, frequently much of the soft tissue in the image (including locations where fine details are important) is misclassified as fluid.

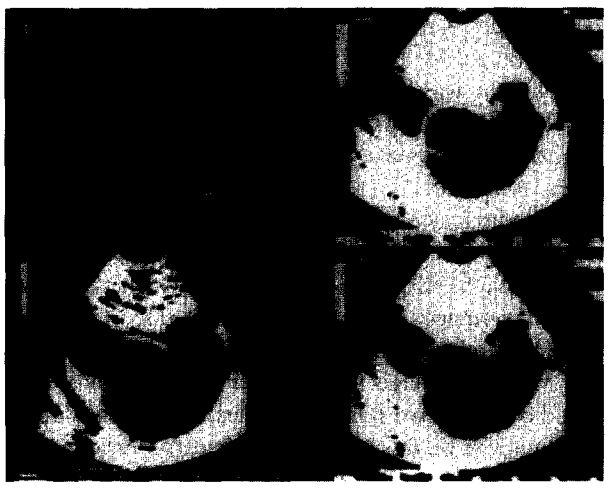

Fig. 3. Segmentation results for an ovarian cyst with transparent fluid (example 2).

Fig.4. Segmentation results for an ovarian cyst with transparent fluid (example 3).

Thresholding the local entropy, on the contrary, provides overestimated bright regions. This is because windows selected near the boundary take into account pixels from both tissues, and also since the fluid near the boundary frequently contains regions of brighter pixels. Both options, which result in a wide local intensity histogram, relate the boundary to large values of the local entropy. Hence, parts of the boundary region are misclassified as bright tissue.

The proposed 2D MCE algorithm seems to provide the best results in most cases. A clear example is Fig. 3, where fine details of the fluid-tissue boundary are lost both in the bottom-left and the top-right images. The images obtained using 2D MCE show a small degree of overestimation in the soft tissue. The effect can be reduced by peeling off several layers of bright pixels near the boundaries. This can be easily performed using, for example, morphological operators such as erosion. Further investigation is obviously required to enable a quantitative use of the obtained results. In those cases where conventional MCE seems to be equal or superior to 2D MCE (e.g., Fig. 4) it is worthwhile to observe that the segmented image after 1D MCE "preserves" the textural properties of the image (i.e., the white regions are full of discontinuities in a pattern similar to the original texture). The binary image obtained from 2D MCE, on the contrary, demonstrates much more homogeneous bright regions. When further image processing steps (e.g., boundary

extraction or shape classification), rather than a simple display, are to follow segmentation, the result obtained from using 2D MCE might be considered better.

Although the proposed algorithm was primarily designed for completely dark fluid, we have tested it also on cysts containing fluid full of small scatterers (bright spots). Figure 5 demonstrates the results obtained for turbid fluid. The structure of this figure is identical to that of Figs. 2–4. We found that, for cysts containing dark fluid with bright spots, conventional MCE (which is equivalent to 2D MCE with zero weight to the local entropy) is optimal.

It is generally expected that 2D MCE will have only limited use for images which demonstrate low contrast between the different tissues (e.g., solid ovarian masses), because in such images the local entropy distributions of the various tissues partially or completely overlap. However, when the ovarian mass contains cystic areas although it is predominantly solid, applying 2D MCE may still be advantageous for specific tasks.

We have also tested the proposed 2D extension using the formulas presented by Brink and Pendock (1996) and found that the results obtained were almost identical to those based on the expression provided by Li and Lee (1993). We can therefore regard both algorithms as equivalent.

In order quantitatively to assess the performance of the proposed method, we compared the results obtained (using 2D MCE with equal weights) with those of an experienced observer. The observer was unaware of the results provided by the automatic algorithm, seeing only the original ultrasound images (before segmentation). After short training (on an image not involved in the comparison), the observer manually outlined the boundaries of the cysts presented in Figs. 2–5. In case the cyst expanded beyond the sector, the boundary of the sector was traced. The region representing each cyst was then obtained by filling the cavity encircled by each outlined boundary.

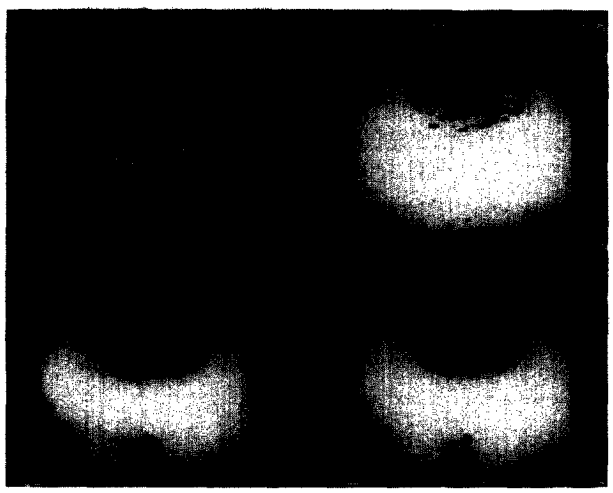

Fig. 5. Segmentation results for an ovarian cyst with turbid fluid.

As demonstrated in Figs. 2–5, the cysts in the automatically segmented images frequently merge either with other dark regions within the imaged sector or with the region outside it. To obtain a cyst, we manually bridged the gaps in its bounding curve, hence forming a closed contour. This was performed either by bridging small gaps in the boundary (e.g., the right side of the cysts in Fig. 2) or by tracing the boundary of the sector and continuing the apparent edges of the cyst until this boundary (e.g., the left side of the cyst in Fig. 3). From these closed curves, the regions representing each cyst are easily obtained. In the future, the closed boundaries should be obtained automatically (e.g., by outlining the boundary of the sector and applying a morphological closing operator with a large window size).

Using the images obtained, we compared the size (i.e., area) of each cyst resulted from manual tracing to the size provided by automatic segmentation. We found that the manually-obtained cyst was always slightly larger than the automatically-generated one; for all four cases (Figs. 2–5), the observed underestimation was in the range 5–7% (taking the manual result as 100%). The difference can be visually interpreted as a 2-to-3-pixel-thick boundary layer. These quantitative results are encouraging, especially when computing the volume of the cyst (using a series of images) is set as the ultimate goal.

The above results, demonstrated in Figs. 2–5, indicate that MCE (including its conventional and 2D versions) segments the images reasonably well. Bivariate (i.e., 2D) MCE is preferred when uniform regions and fine (or faint) details are extremely important; conventional MCE is selected when small bright spots are not desired (turbid fluid) or when we wish to preserve the "natural" texture of the image. Applying 2D MCE with unequal weights may provide a general solution to a wide variety of image properties and user requirements. Hence, although no general improvement was observed for unequal weights, this aspect of the subject should be further investigated. An additional effort should also be made to find other variables suitable for segmentation, leading to multi-dimensional MCE. Additional directions of future work can be: quantitative examination of the effects of window size and of ROI on the results, segmentation of smoothed images, application of 2D MCE on images describing other organs or obtained using other im-

aging modalities, and derivation of multi-dimensional extensions of other thresholding techniques.

SUMMARY

In this article, a multi-dimensional extension of MCE has been presented. The new version replaces the segmented variable (gray level) by a weighted combination of several image parameters. We proposed to use a 2D extension of MCE, which uses a linear combination of the gray level and the local entropy, to segment ultrasound images containing fluid surrounded by a soft tissue. The algorithm was tested on ultrasound images of ovarian cysts. For cysts containing transparent fluid, bivariate MCE usually segmented the images better than univariate (conventional) MCE. Several aspects of the subject should be further investigated.

Acknowledgements—This research is supported by a grant from the Ministry of Science, and by the Abramson Center for Medical Physics.

REFERENCES

Abutaleb AS. Automatic thresholding of gray-level pictures using two dimensional entropy. Comput Vision Graphics Image Process 1989;47:22–32.

Brink AD. Thresholding of digital images using two-dimensional entropies. Pattern Recognition 1992;25:803–808.

Brink AD, Pendock NE. Minimum cross entropy threshold selection. Pattern Recognition 1996;29:179–188.

Crawford DC, Bell DS, Bamber JC. Compensation for the signal processing characteristics of ultrasound B-mode scanners in adaptive speckle reduction. Ultrasound Med Biol 1993;19:469–485.

Kapur JN, Sahoo PK, Wong AKC. A new method for gray-level picture thresholding using the entropy of the histogram. Comput Vision Graphics Image Process 1985;29:273–285.

Karaman M, Kutay MA, Bozdagi G. An adaptive speckle suppression filter for medical ultrasonic imaging. IEEE Trans Med Imaging 1995;14:283–292.

Kittler J, Illingworth J. Minimum error thresholding. Pattern Recognition 1986;19:41–47.

Kullback S. Information theory and statistics. New York: John Wiley & Sons, 1959.

Li CH, Lee CK. Minimum cross entropy thresholding. Pattern Recognition 1993;26:617–625.

Muzzolini R, Yang YH, Pierson R. Multiresolution texture segmentation with application to diagnostic ultrasound images. IEEE Trans Med Imaging 1993;12:108–123.

Muzzolini R, Yang YH, Pierson R. Texture characterization using robust statistics. Pattern Recognition 1994;27:119–134.

Otsu N. A threshold selection method from gray-level histogram. IEEE Trans Syst Man Cybern 1979;9:62–66.

Shinozuka N, Oye Y, Yamakoshi Y, Taketani Y. Transvaginal sonographic orientation detection system using ceramic gyroscopes. J Ultrasound Med 1996;15:107–113.